Journal of Food Engineering 199 (2017) 42–53

Contents lists available at ScienceDirect

Journal of Food Engineering

journal homepage: www.elsevier.com/locate/jfoodeng

Storage-induced caking of cocoa powder

J. Petit [a], F. Michaux [a], C. Jacquot [a], E. Chávez Montes [b], J. Dupas [b], V. Girard [b], A. Gianfrancesco [c], J. Scher [a], C. Gaiani [a, *]

[a] Université de Lorraine, Laboratoire d'Ingénierie des Biomolécules (LIBio), 2, avenue de la Forêt de Haye, TSA 40602, 54518 Vandœuvre-lès-Nancy, France
[b] Nestlé Product Technology Center, 1350 3, route de Chavornay, Switzerland
[c] Nestlé Research Konolfingen, Nestléstrasse 3, 3510 Konolfingen, Switzerland

ARTICLE INFO

Article history:
Received 31 May 2016
Received in revised form
29 November 2016
Accepted 7 December 2016
Available online 13 December 2016

Keywords:
Cocoa powder
Caking
Storage
Fat migration
Surface composition
Particle structure

ABSTRACT

Cocoa powders are highly subjected to caking, a phenomenon of solid particles agglomeration that impairs powder functionalities such as rehydration and flowing properties. This study aimed at identifying the main caking mechanisms occurring during storage of cocoa powders, according to their fat content and water activity, as well as storage temperature. The formation of caked powder was monitored at macroscopic scale by sieve analysis, showing that caking was significant only for fatty powders at 40 °C, in agreement with a caking mechanism controlled by fat melting. The similarity of results obtained at 0.2 and 0.7 water activity indicated that the humidity caking mechanism was not significant for these powders. Observations performed by TEM evidenced the formation of fat bridges, confirming the occurrence of the fat melting mechanism. Then, solvent extraction techniques designed to quantify fat fractions permitted to highlight that storage caused the conversion of encapsulated fat into free fat. At temperatures sufficient to melt cocoa fat (40 °C), this newly formed free fat migrates toward cocoa particle surface, enhancing its fat coverage, hence making cocoa particle sticky and prone to cake. Finally, XPS analysis of the extreme surface of cocoa powders confirmed that two conditions should be met to trigger significant cocoa powder caking: high fat content and elevated storage temperature.

1. Introduction

In the literature, researches on cocoa powders have mainly focused on their health benefices: neuroprotective (Cimini et al., 2013), antioxidant, antimicrobial (Calatayud et al., 2013), cardioprotective activities (Abdi et al., 2013), etc. These health benefices are related to cocoa polyphenols, which are large biomolecules highly sensitive to photo- or thermal oxidation. Thus, cocoa powder processing and storage must be carefully carried out in order to limit bioactive compound and physical properties alterations. The lack of literature studies linking cocoa powder properties to process or storage conditions shows that the understanding of cocoa powder caking during storage requires investigating the impact of storage conditions on cocoa powder structure and surface composition, as well as on their other physicochemical properties (like particle size and shape distributions, fat composition, etc.).

Few works dealing with cocoa powder ageing can be found in the literature. Nevertheless, numerous studies have been published about storage-induced defects of chocolate, mainly those related to polymorphic changes occurring in cocoa fat (Altimiras et al., 2007; Bricknell and Hartel, 1998; Peschar et al., 2004; Tietz and Hartel, 2000): fat bloom, sugar bloom, and swelling. Briefly, fat bloom corresponds to the formation of a white deposit of small fat crystals on the product surface (Hartel, 1999), impairing chocolate visual appearance and texture (Briones and Aguilera, 2005); sugar bloom reflects sugar crystallisation induced by variations of surrounding air humidity and leads to an unpleasant dusty appearance of chocolate surface; and swelling, mostly affecting chocolate texture, is triggered by moisture uptake from the surrounding air and results from water migration, dependently of fat migration and local polymorphic changes (Svanberg et al., 2012).

Chocolate is a product made with cocoa liquor (containing cocoa butter and cocoa solids), with some technological additives and other ingredients in lower proportions. As cocoa powder, obtained from the pressing of cocoa liquor, still contains cocoa butter in variable amounts, it can be assumed that comparable storage-induced defects may occur in cocoa powder and chocolate. Incidentally, these defects can be limited by tempering cocoa-

* Corresponding author.
E-mail address: claire.gaiani@univ-lorraine.fr (C. Gaiani).

http://dx.doi.org/10.1016/j.jfoodeng.2016.12.005
0260-8774/

containing products, which consists in lipid crystallisation (leading to a stable physical state) performed with meticulous time-temperature schedules (Afoakwa et al., 2007; Lonchampt and Hartel, 2006; Talbot, 1999).

Caking designates the formation of a solid bridge between two particles in contact, which is generally the consequence of the solidification of a liquid bridge (Foster, 2002). Caking induces the alteration of food powder use and handling properties (aptitude to reconstitution, agglomeration, handling, conveying, packaging, etc.) (Le Brun et al., 2006). Powder caking is mainly due to a sintering mechanism, i.e. molecular diffusion from amorphous particles to contact zone between particles, driven by the reduction of the surface of particles at constant volume and resulting in a decrease in free energy of the system (Aguilera et al., 1995; Hartmann and Palzer, 2011). Other mechanisms include melting/crystallization of lipids, sugars, or minerals. The particle shape is deeply modified by caking, unless if particles possess an insoluble backbone (e.g., cellulose, silicates, fat, proteins) (Hartmann and Palzer, 2011). Crystallisation may induce water release (like in the case of conversion of monohydrated amorphous lactose into crystallised form), which enhances caking by liquefying local areas of powders, allowing the formation of liquid bridges (Hartmann and Palzer, 2011). Four caking mechanisms, depending on powder composition and environmental conditions, have been identified in the literature for food powders (Foster, 2002): amorphous sugar caking, humidity caking, fat melting caking, and caking caused by protein sticking. Amorphous sugar caking, mostly occurring in hygroscopic powders of amorphous structure, corresponds to the transition from glassy to rubbery state of amorphous sugars when moisture content or temperature is increased, leading to higher particle stickiness and making powders prone to cake. Humidity caking, subsequent to water uptake, consists in water sorption/condensation at the particle surface, inducing the dissolution of surface components up to saturation and the formation of liquid bridges between particles; the latter transform into solid bridges under the action of drying, i.e. when temperature is increased or surrounding air humidity is decreased. Fat melting caking results from the formation of liquid bridges of fat over its melting point (as liquid fat is very sticky), which crystallise when temperature is decreased. Last, protein denaturation and aggregation at elevated temperature may increase particle stickiness and cause powder caking. Cocoa powders, which are highly hydrophobic owing to their large fat content (Omobuwajo et al., 2000), are expected to be affected by the humidity and fat melting caking mechanisms mostly.

Caking induces the formation of powder lumps: at a given caking stage, lumps may be few or numerous, of different sizes and of various degrees of hardness (Aguilera et al., 1995), hence the difficulty to define a unique representative parameter for caking and to monitor caking phenomenon during powder processing or storage. The major analytical techniques for monitoring powder caking are sieve analysis, which permits to quantify the fraction of agglomerated particles, compression tests of a consolidated powder cake, and shear tests of a powder bed under compression, which evaluate the caking-induced decrease in powder flowability (Aguilera et al., 1995; Le Brun et al., 2006).

In this work some physicochemical factors and storage conditions influencing caking of cocoa powders were studied. Three cocoa powders differing in fat content (1, 11, and 21%) were stored in various storage conditions during 2 months. Three storage temperatures (20, 30, and 40 °C) and two surrounding air relative humidities (20% and 70%) were employed to investigate the influence of temperature and water activity on cocoa powder caking, depending on fat content. Structural changes caused by storage in these different conditions were characterised by a multiscale approach. At macroscopic scale, caking was quantified by a sieving procedure. At microscopic scale, mean particle size and shape distribution were evaluated by laser granulometry and morphogranulometry, cocoa powders were imaged by TEM in order to give insight into fat location in particles, and total fat content, along with the distribution of fat within free and encapsulated fractions, were determined by solvent extraction methods. Lastly, at molecular scale, XPS analyses permitted to discuss the evolution of surface fat according to storage conditions. The final objective of this study was to identify the main caking mechanism(s) acting in cocoa powders according to storage temperature and water activity.

2. Material and methods

2.1. Cocoa powders and storage conditions

The influence of fat content on cocoa powder caking was investigated by studying the storage behaviour of three cocoa powders differing in fat content manufactured by De Zaan Cocoa (ADM Cocoa, Rolle, Switzerland):

- defatted (<0.5% fat) alkalised cocoa powder D-00-ZR, called CP1,
- 10–12% fat alkalised cocoa powder D-11-SB, referred as CP11,
- 20–22% fat alkalised cocoa powder D-21-S, named CP21.

Their composition in macronutrients (supplied by Olam Cocoa B.V., Koog aan de Zaan, the Netherlands) is presented in Table 1. Investigated cocoa powders markedly differed in fat content, whereas moisture, theobromine, and caffeine were present in quite similar amounts. Protein, carbohydrate, dietary fibre, and ash contents decreased when increasing the fat content.

Cocoa powders were gently poured in polystyrene Petri dishes (60 mm × 15 mm) so as to form a particle layer of circa 1 cm and stored at controlled temperature and water activity during 56 days. The influence of temperature on caking mechanisms was investigated by storing cocoa powders in hermetically-closed boxes placed in thermostated enclosures regulated at 20, 30, and 40 °C, the latter temperature being considered as critical for complete melting of cocoa butter fat (Jacquot et al., 2016; Wille and Lutton, 1966).

For all temperatures, a potassium acetate (CH_3COOK) saturated saline solution was employed to set powder water activity (a_w) at about 0.2 during storage in hermetically-closed boxes. The influence of water activity on cocoa powder storage-induced caking was investigated at 20 °C by using a potassium iodide (KI) saturated saline solution, fixing the water activity at about 0.7.

All samples have been analysed in triplicates (except for XPS analyses, cf. section 2.3.2) at different storage times up to 56 days.

2.2. Caking monitoring during storage

2.2.1. Powder sieving and caking index

Powder caking was first tracked at macroscopic scale by following the evolution of the fraction of caked powder during storage. To this end, a caking index was defined and determined by sieve analysis, with the purpose of validating a quick and simple tool to put in evidence powder caking.

Powder samples were separated into different granulometric fractions with the vibratory sieve shaker Analysette 3 Spartan (Fritsch, Idar-Oberstein, Germany) at 0.5 mm vibration amplitude for 30 s in permanent mode. Approximately 100 g of powder were initially placed on the top sieve. 20 mm diameter sieves (Fritsch) were employed so as to obtain the following granulometric fractions: > 500 μm; 315–500 μm; 180–315 μm; 100–180 μm; 50–100 μm; 20–50 μm; < 20 μm. Each fraction was weighed to

determine the mass fractions of granulometric classes, used to calculate the caking index according to GEA Niro's method (GEA Niro Research Laboratory, 2003). In this study, the most relevant sieve opening for the calculation of caking index was found at 315 μm, leading to the formula given in equation (1):

$$CI = \frac{m_{>315\mu m}}{m_{tot}} \quad (1)$$

where $m_{>315\mu m}$ is the powder mass retained on the 315 sieve and m_{tot} the total mass of analysed powder.

Caking indices at 180 μm and 500 μm were also considered, but they were less suitable to describe the evolution of cocoa powder caking. Indeed, some cocoa particles were larger than 180 μm at fresh state (i.e. at the beginning of the storage), leading to elevated values of the 180 μm caking index for all storage times. Besides, too few caked particles were bigger than 500 μm even after 56 days storage, resulting in almost no evolution of the 500 μm caking index during storage.

2.2.2. Particle size and shape distributions

Particle size distributions of cocoa powders were evaluated by laser granulometry (Mastersizer S, Malvern Instruments, Orsay, France) at room temperature. The appropriate quantity of sample was dispersed in ethanol (95%) to reach between 16% and 20% obscuration. Ethanol was chosen as dispersing medium to limit particle rehydration and allow proper dispersion of cocoa particles during analysis. Particle stability during analysis was validated by successive measurements during 20 min (data not shown), showing no significant evolution of particle size distributions and ensuring method accuracy. Mean particle size in volume D_{50} was chosen as size estimator.

Particle shape distributions of cocoa particles were determined with the Qicpic™ morphogranulometer (Sympatec GmbH, Clausthal-Zellerfeld, Germany) supplied with a Lixell module (Sympatec GmbH) connected to a small reactor (200 mL) with a peristaltic pump. Windox software (Windox 5.4–2007, Sympatec GmbH) was used to convert acquired images into particle size and shape distributions. For each analysis, approximately 0.25 g powder sample was suspended in 75 mL ethanol in order to attain a proper obscuration of about 5% and avoid particle superimposition. The diameter of a circle of equal projection area (EQPC), defined as the diameter of a circle that has the same area as the projection of the particle, was chosen as size estimator. Finally, the mean sphericity of particles was calculated from particle images as the ratio between the EQPC perimeter and the real perimeter of a particle, leading to values ranging from 0 to 1. A more irregular particle shape corresponds to an increase in real perimeter at fixed EQPC; thus, the more irregular the particle shape, the lower its sphericity.

2.3. Total, free, encapsulated, and surface fat

In order to relate caking ability to the presence of fat at the surface of cocoa powder particles, two approaches were followed: on one hand, total, free, and encapsulated fat of cocoa particles were determined by solvent extraction; on the other hand, XPS analysis of particle surface was performed to identify lipids through specific atomic and chemical bond signatures, i.e. the C/O ratio and the C–C(H) bond proportion within C bonds (Jacquot et al., 2016).

Table 1
Chemical composition of fresh cocoa powders.

Cocoa Powder	CP1 (%)	CP11 (%)	CP21 (%)
Fat	0.5	11.0	21.0
Protein	24.4	22.0	18.1
Theobromine	2.3	2.1	2.5
Caffeine	0.2	0.2	0.1
Carbohydrates	54.9	48.7	44.8
- incl. Dietary fibers	35.5	31.6	28.0
Ash	13.7	12.0	9.5
Moisture	4.0	4.0	4.0

Contents were expressed in weight percentages in wet basis.

2.3.1. Solvent extractions of fat

Fat extraction techniques developed for other food powders (Gaiani et al., 2007a; Murrieta-Pazos et al., 2012b; Vignolles et al., 2007) were adapted to cocoa powders in a previous work (Jacquot et al., 2016). The mass proportions of each fat fraction were expressed on dry basis, i.e. in g per 100 g dry matter.

2.3.1.1. Free fat extraction. Free fat was extracted from 10 g of cocoa powder, which were weighed in a previously dried Erlenmeyer flask. 50 mL petroleum ether was added before stirring at 200 rpm during 1 min. Then, the solvent was removed by filtration (Whatmann n°2 filter) and the permeate was recovered in a round-bottom boiling flask that was previously dried and weighed. The solvent was then removed with a rotary vacuum evaporator (Heidolph Laborota 4000) at 40 °C and 40 rpm. The remaining permeate was dried in an oven at 103 °C for 10 min to ensure complete solvent evaporation and lastly weighed. Finally, the free fat percentage was calculated by weight difference.

2.3.1.2. Total fat extraction. Total fat extraction was performed with a method adapted from (Folch et al., 1957). 10 g cocoa powder was dissolved in chloroform/methanol (2:1 (v/v)). The mix was stirred at 700 rpm during 15 min. Solvent separation and fat fraction recovery were carried out as described in the previous subsection.

2.3.1.3. Encapsulated fat extraction. Encapsulated fat was measured from the total fat fraction remaining in the cocoa particle after free fat extraction. Encapsulated fat quantification was performed by applying the total fat extraction method on the retentate obtained during free fat extraction, i.e. partially defatted powder recuperated on the filter.

2.3.2. XPS analysis: surface composition

Surface elemental composition of cocoa powders (up to 5–10 nm depth) was analysed by X-Ray Photoelectron Spectroscopy (XPS). The suitability of this technique for analysing cocoa powders surface was demonstrated in a previous work (Jacquot et al., 2016), and its application on cocoa powders benefits from the analytical experience acquired on other food powders (Gaiani et al., 2006; Murrieta-Pazos et al., 2012a; Nikolova et al., 2014) or chocolate products (James and Smith, 2009). XPS provides elemental and chemical state data of solid samples. The sample, placed in ultra-high vacuum (10^{-8} Pa), is irradiated with photons from a soft X-ray source of well-defined energy, which is completely transferred to atomic electrons of the sample. When the electron binding energy (E_b) is lower than the photon energy ($h\nu$), the electron is emitted from the atom with a kinetic energy (E_k) equal to the difference between the photon kinetic energy and the electron binding energy minus the spectrometer work function Φ (equation (2)):

$$E_k = h\nu - E_b - \Phi \quad (2)$$

In this study, XPS analysis was carried out with a Kratos Axis Ultra (Kratos Analytical, Manchester, UK) photoelectron spectrometer, which uses a monochromatic Al K_α X-ray source. Cocoa powder samples were attached to a sample holder with a double-side conductive tape for analytical purposes. Fresh and aged

samples were analysed only twice and once, respectively, owing to the high cost and duration of XPS analysis. Spectra were analysed using the Vision 2.2.0 software (Kratos). Quantification of atomic composition (in C, O, N, K, and P) and carbon chemical bond was performed using the photoemission cross-sections and transmission coefficients given in the Vision package. Atomic composition was deduced from the peak area corresponding to each atomic signature (C_{1s}, O_{1s}, N_{1s}, K_{2p}, and P_{2p}), whereas carbon bonds were quantified by deconvolution of C_{1s} peak into C–C,H; C–O,N; C═O; O–C═O bonds.

2.4. Powder imaging by TEM analysis

For Transmission Electron Microscopy (TEM) analyses, powders were first dehydrated in ethanol and propylene oxide. Then, cocoa powders were pre-impregnated in a mixture of Epon embed 812 resin (2/3) and propylene oxide (1/3) during 5 h and finally included in pure resin during 16 h. Resin polymerisation was finally performed at 56 °C for 48 h. Thin slices (80 nm) were coloured and contrasted in 3% uranyl acetate aqueous solution and Reynolds coloration. Slices were put on copper grids covered with carbon film. Finally, examinations were carried out with a CM12 microscope (Philips, Amsterdam, Netherlands) operating at 80 kV.

3. Results and discussion

3.1. Caking monitoring at macroscopic scale

Cocoa powder caking can be monitored all along the storage by calculating the caking index at 315 μm from the sieving procedure (Fig. 1). Fig. 1 confirms the suitability of the caking index for evidencing the caking phenomenon during powder storage in controlled conditions: indeed, it can be seen on Fig. 1B (CP11) and 1C (CP21) that CI initial values were close to zero (very few initial particles were greater than 315 μm), which corresponds to the absence of caking. This parameter increased with time in certain storage conditions (cf. Fig. 1B and 1C), showing the occurrence of cocoa powder caking. Unfortunately, the sieving procedure was unsatisfying for CP1, leading to large values and great uncertainties all along the storage (cf. Fig. 1A). It was stated that the quasi absence of lipids in CP1 (cf. Table 1) was associated with a higher surface roughness, leading to electrostatic agglomeration of powder particles during sieving, owing to friction with sieve walls and grids. This hypothesis was supported by sphericity results, as shown in section 3.2.

Significant storage-induced caking was observed for CP11 and CP21 powders at 40 °C only, showing that both high fat content and elevated temperatures are needed for substantial powder caking, suggesting a strong influence of the fat melting mechanism on cocoa powder caking in accordance with other studies (Altimiras et al., 2007; Chávez Montes et al., 2011; Foster, 2002; Omobuwajo et al., 2000). At 30 °C, 10% CI only was obtained for CP21 after 56 days storage (cf. Fig. 1C), showing that the threshold temperature for cocoa powder caking may be found between 30 and 40 °C. No influence of storage water activity was denoted (cf. triangles in Fig. 1), suggesting that the humidity caking mechanism may not be influent during storage of cocoa powders. CP11 caking index at 40 °C was substantially increased from the first storage time, reaching a plateau at 60–70% CI after about 15 days. CP21 caking at 40 °C developed faster, reaching high values in the first storage days, fluctuating until 15 days, and finally stabilising around 30–40% CI. Caking index evolutions differed for CP11 and CP21, suggesting that particle characteristics (size, shape, surface composition, etc.) may play a role of utmost importance in storage-induced caking of cocoa powders. Particle size and shape results, as well quantification of total, free, and encapsulated fat fractions helped adjudicating this question in the following sections 3.2 and 3.3.1.

3.2. Caking-induced structural modifications at particle scale

The evolutions of mean particle size D_{50} with storage time for all cocoa powders and storage conditions were drawn in Fig. 2. Particle size distributions of fresh and aged cocoa powders were bimodal, with a major population ranging between 1 and 100 μm and a minor one between 0,1 and 1 μm (see Fig. S1 in Supplementary material). Initial particle size differed between cocoa powders: it increased with fat content (8.14 ± 0.02 μm for CP1, 13.38 ± 0.13 μm for CP11, 30.18 ± 0.17 μm for CP21). The presence of fat seems to be crucial, as no particle size increase was observed for the defatted powder (CP1) during storage, contrarily to CP11 and CP21 that contained significant amounts of fat and experienced small increases in particle size at 40 °C (cf. Fig. 2B and C). A very small particle size increase could also be noticed for CP21 after 56 days storage at 30 °C. Fig. 2 These results indicate that a temperature threshold between 30 and 40 °C can be defined for the triggering of particle size increase. Indeed, mean particle size of all powders, whatever their fat content, remained globally stable at 20 and 30 °C, whereas moderate increases in D_{50} from 13.38 ± 0.13 to 15.99 ± 0.20 μm (+19.5%) and from 30.18 ± 0.17 to 35.18 ± 1.03 μm (+16.5%) after circa 15 days storage at 40 °C were observed for CP11 and CP21, respectively. Particle sizes obtained from laser granulometry were well smaller than agglomerate sizes determined by sieve analysis (cf. Figs. 1 and 2, and Fig. S1), meaning that particle agglomerates were disrupted during laser granulometry analysis, likely due to dispersion in ethanol. Thus, observed particle size increases were caused by changes of particle inner structure during storage. The temperature threshold for particle size increase, found between 30 and 40 °C, may be related to the fact that melting points of cocoa lipids are below 40 °C (Wille and Lutton, 1966): particle size increase probably resulted from fat migration toward particle surface. This hypothesis is supported by the shift to the right of particle size distributions (Fig. S1), as the observation of agglomerates in laser granulometry would have induced the apparition of a new peak (corresponding to agglomerates) of large particles.

In a previous work (Jacquot et al., 2016), it was shown by DSC measurements that cocoa lipids of CP11 melt between 25 and 35 °C, with peak value at 32 °C. Peak integration led to a proportion of circa 33% molten fat at 30 °C and the same proportion was similarly obtained for CP21 (data not shown). Thus, the fact that particle size increase and powder caking both occurred significantly at 40 °C for CP11 and CP21 but only slightly at 30 °C for CP21 (cf. Fig. 1B and C) is in total agreement with a major role of molten fat in cocoa powder caking. In few words, less molten lipids (at 30 °C) induced lower particle size increase and less powder caking. Besides, remaining solid lipids (for instance at 30 °C) can block the exit of open pores and hinder migration of molten lipids, leading to less caking than expected on the single basis of the proportion of molten fat: this may explain the very low caking index of CP21 at 30 °C (Fig. 1C) and its small (+5.4%) size increase from 30.18 ± 0.17 μm (fresh CP21) to 31.81 ± 0.16 μm (CP21, 56 days, 30 °C), in spite of the significant proportion of molten fat (33%) (cf. Fig. S1 in the Supplementary material).

Whatever the considered cocoa powder, water activity did not influence the evolution of particle size, confirming that the humidity caking mechanism do not play a significant role in fat migration or cocoa powder caking (Chávez Montes et al., 2011). This is consistent with the fact that the humidity caking mechanism mainly concerns highly hydrophilic powders (Aguilera et al., 1995;

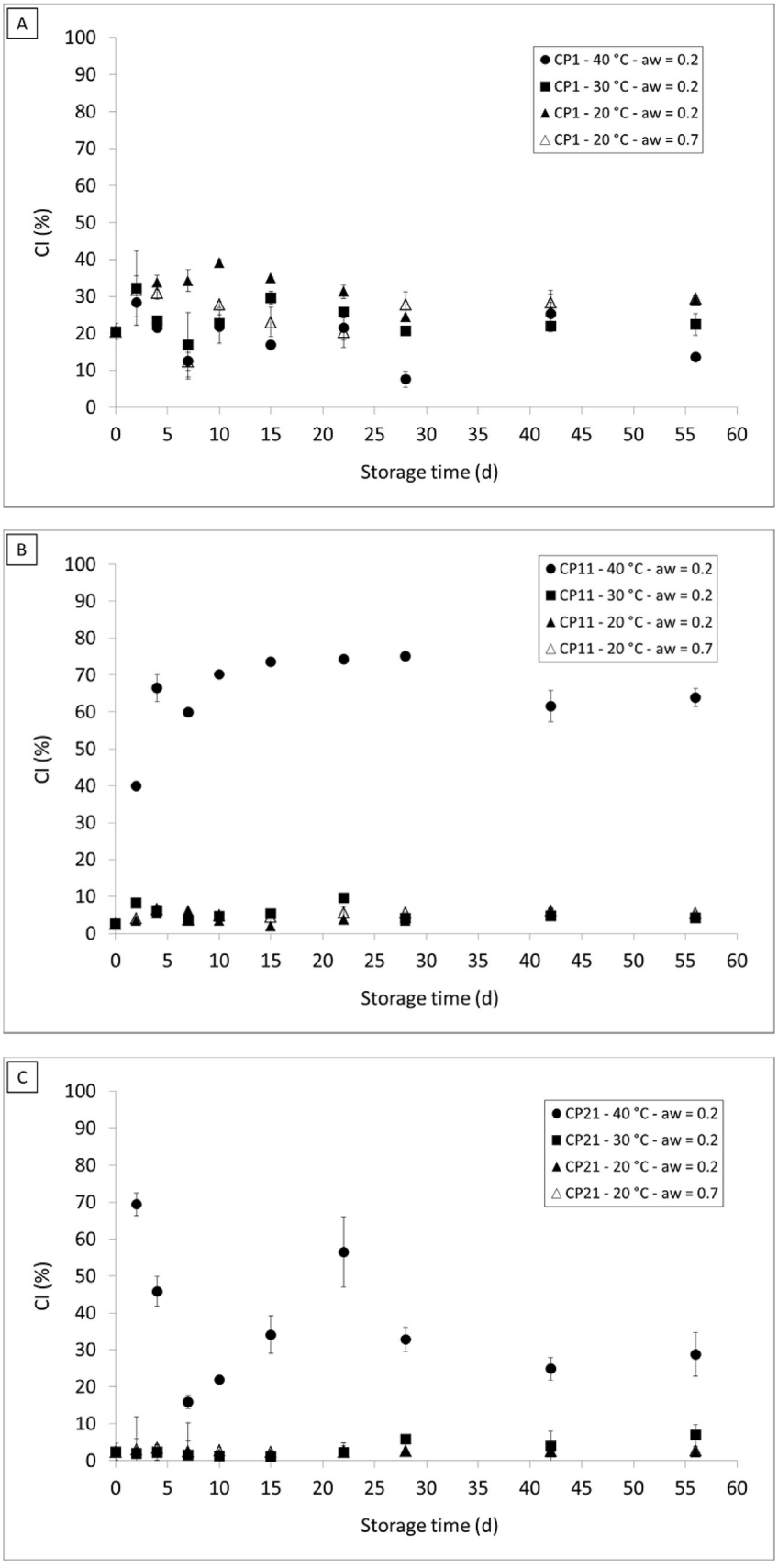

Fig. 1. Evolution of caking index of cocoa powders with storage time. **A**: CP1; **B**: CP11; **C**: CP21. When not visible, standard errors were inferior to the marker size.

Foster, 2002).

Changes in particle sphericity (Fig. 3) may also be linked to powder caking during storage. Different behaviours for defatted and fat-containing cocoa powders can be observed on Fig. 3 For CP1, storage at 40 °C induced a small decrease in sphericity in the whole particle size range. This unspecific change in particle shape, which was independent from fat melting as CP1 contains only residual amounts of fat, may be related to physicochemical rearrangements of powder structure caused by equilibration with air relative humidity. Indeed, plant fibres are known to be hydrophilic and have a great tendency to bind water (Célino et al., 2014). During storage, food powders and surrounding air equilibrate, i.e. the water activity of food powders tends toward air relative humidity and vice versa. This occurs by water exchange between food powder and surrounding air. In powders having such a high fibre content (about 30% on wet basis, cf. Table 1) as investigated cocoa powders, the absorption (resp., release) of water by fibres owing to equilibration during storage may induce their swelling (resp., shrinkage). Swelling and shrinkage phenomena are responsible for internal stresses within particles (Célino et al., 2014), which alter particle structure by creating surface cracks and new internal pores, opening closed pores, and/or increase surface roughness (thus decreasing particle sphericity, as recently evidenced by Burgain et al. (2016) for dairy powders). Consequently, structural changes

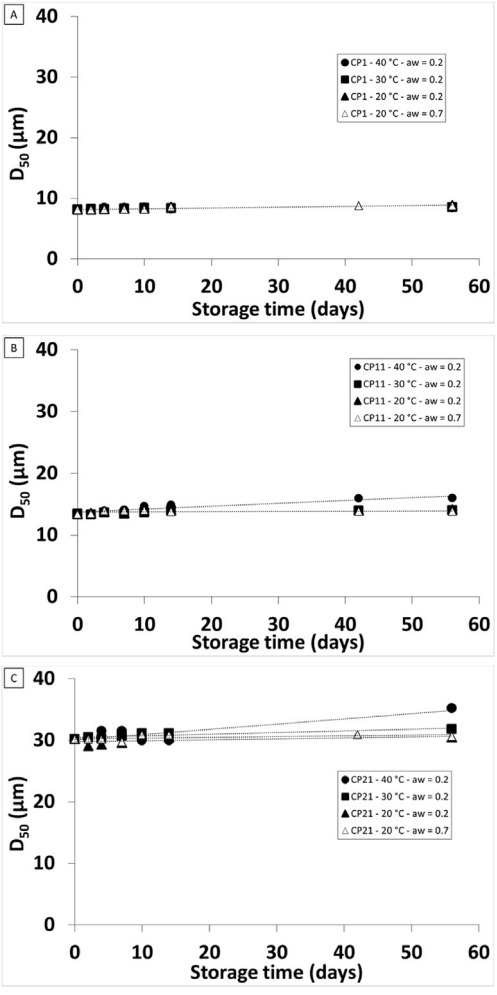

Fig. 2. Evolution of mean particle size D_{50} of cocoa powders with storage time. **A**: CP1; **B**: CP11; **C**: CP21. Dotted curves were added to highlight discrepancies between particle size evolutions. Standard errors were inferior to the marker size.

were expected for investigated powders in all storage conditions. Moreover, lipid density being inferior at liquid state than at solid state, the melting of cocoa lipids (occurring between 25 and 35 °C, Jacquot et al., 2016) should also contribute to the formation of cracks and/or the opening of closed pores: indeed, in closed pores, the melting of enclosed fat increases internal pressure, inducing mechanical stresses in pore walls, which can result in pore deformation and opening. This phenomenon requires that temperature exceeds the melting points of some cocoa lipids (hence in cocoa powders stored at 30 and 40 °C) and fat content is sufficient (i.e. for CP11 and CP21).

Besides, Fig. 3 shows that CP1 particles were less spherical than CP11 and CP21 ones, making CP1 more sensitive to electrostatic effects in sieve analysis, in agreement with the previously mentioned analytical issues encountered in CP1 sieve analysis (cf. section 3.1).

As for CP11 and CP21, it is remarkable that CP21 particles (squares in Fig. 3) were systematically more spherical than CP11 ones (triangles in Fig. 3) both for fresh (full markers) and aged (empty markers) powders, whatever the particle size. Particle shape is expected to have a tremendous impact on particle agglomeration mechanisms, as illustrated by Fig. 4. More spherical particles are expected to have less contact points between them and thus to form less bridges if agglomeration conditions are met. Indeed, more spherical particles are generally more compact, which limits mechanical interlocking between particles and further agglomeration. This effect of particle shape is independent from the particle size, as sketched in Fig. 4. Thus, the higher sphericity of CP21 particles compared to CP11 ones (cf. Fig. 3) could explain why CP21 was less sensitive to caking than CP11. Incidentally, size is expected to have a positive effect on particle ability to form bridges, by increasing the number of possible contact points (Fig. 4). The current study did not allow evidencing this stated influence of particle size (as CP11, although constituted by smaller particles, was more affected by storage-induced caking than CP21, cf. Fig. 1B and C), suggesting a higher influence of particle shape of cocoa powders in their caking ability.

Moreover, no change in sphericity was detected for other storage temperatures and it was noted that the alteration of particle shape was similar whatever the powder water activity during storage (data acquired at 0.7 water activity not shown), confirming the predominance of the fat melting mechanism and the negligible influence of the humidity caking mechanism in cocoa powder caking.

3.3. Storage influence on surface fat content

Now that the relation between particle physical properties (size and shape) and cocoa powder caking has been highlighted, the following of the study focuses on the influence of particle surface composition (in particular, the fraction of fat coverage) on powder sensitivity to caking.

3.3.1. Free, encapsulated, and total fat contents during storage

Consistently with supplier data indicating about 0.5% residual fat in CP1, very low values (within the uncertainty margin) were found for free, encapsulated, and total fat contents of CP1; hence, there is no interest to present these results here in detail. Fig. 5 displays the evolution of fat contents of CP11 and CP21 in investigated storage conditions.

It can be noted on Fig. 5 that the total fat contents of CP11 and CP21 were respectively evaluated at 10.46 ± 0.07 and 19.54 ± 0.06 g per 100 g dry matter, in agreement with supplier data (11.4 and 21.9 g per 100 g dry matter, respectively). No significant evolution of total fat content was denoted during storage, showing the

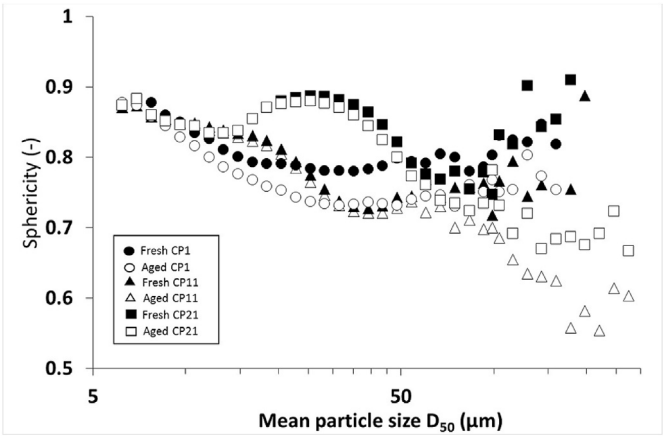

Fig. 3. Influence of storage at 40 °C and 0.2 water activity on cocoa particle sphericity according to particle size. X-axis is in logarithmic scale. Standard errors were inferior to the marker size.

reproducibility of the total fat extraction method. As regards the free fat content corresponding to the fat fraction located either on powder surface, in cracks, or in open pores (Vignolles et al., 2007), a similar trend was obtained for CP11 and CP21 whatever the storage temperature. The free fat content increased from the first storage days, reached a plateau from about 15 days, and remained stable at maximal value (on average for all storage conditions, 9.05 ± 0.10 and 16.57 ± 0.65 g per 100 g dry matter for CP11 and CP21 respectively) after.

From these results, it can be stated that structural modifications (due to fibre swelling/shrinkage and fat melting of cocoa particles, cf. section 3.2) occurred until 10 - 15 storage days, leading to the formation of new open pores from closed ones, thus allowing some encapsulated fat, which was previously confined in closed pores or embedded in powder matrix, to be released in open pores and become free fat. Moreover, the fact that the free fat fraction increased more for CP11 (+50%) than CP21 (+35%) during storage may be another explanation of the higher sensitivity of CP11 to caking. Indeed, surface fat is the fraction of free fat expected to be involved in powder caking, as it plays a major role in the stickiness of cocoa particle surface.

The various storage conditions induced almost no difference in the temporal evolution of fat contents. It can be concluded that the conversion of some encapsulated fat into new free fat occurs whatever the storage conditions at temperatures above ambient, probably because of crack formation and pore opening subsequently to fibre swelling/shrinkage.

In brief, the results obtained by sieve analysis, laser granulometry, morphogranulometry, and solvent extraction of fat fractions led to the conclusion that the main caking mechanism acting during cocoa powder storage is the fat melting mechanism, caused by the presence of molten fat at the surface of fatty cocoa powders when the storage temperature is greater than the melting points of cocoa lipids. Caking seems to be markedly enhanced when free fat is released by transformation of closed pores into open ones subsequent to fibre swelling/shrinkage and fat melting, making the newly free fat able to migrate toward the particle surface and improve particle surface fat coverage and stickiness. Thus, only powders having a significant fat content will cake during storage, on the condition that storage temperature is above 25 °C, the latter being the lower melting point of cocoa lipids (Jacquot et al., 2016; Wille and Lutton, 1966). Substantial caking is thus expected for fatty cocoa powders over 36 °C, which corresponds to the temperature range where cocoa lipids are expected to be completely molten (Jacquot et al., 2016; Wille and Lutton, 1966). This hypothesis allows explaining the more elevated caking index of CP11 in comparison with CP21 after 56 days storage: it derived from the higher increase in free fat of CP11 (i.e. the higher amount of newly formed free fat during storage)associated with higher increase in its surface stickiness. This explanation is also in accordance with the greater variability of CI results for CP21 (see the higher standard errors at 40 °C and 0.2 a_w on Fig. 2C): indeed, less new free fat led to less agglomerated powder but also fewer bridges between particles, making CP21 agglomerates more fragile (hence more sensitive to breaking during sieve analysis) than CP11 ones.

Last, particle size and shape are expected to influence powder caking ability (Fig. 4), as non-spherical and/or large particles have

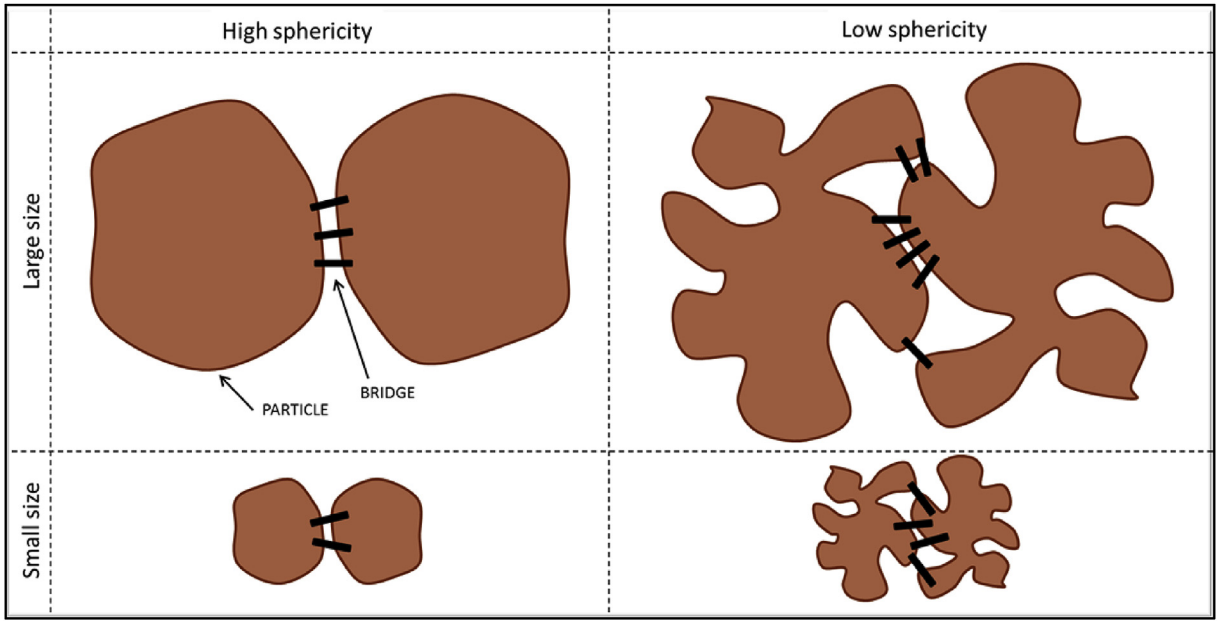

Fig. 4. Schematic representation of the influence of particle size and shape on the ability of powders to agglomerate by bridge formation.

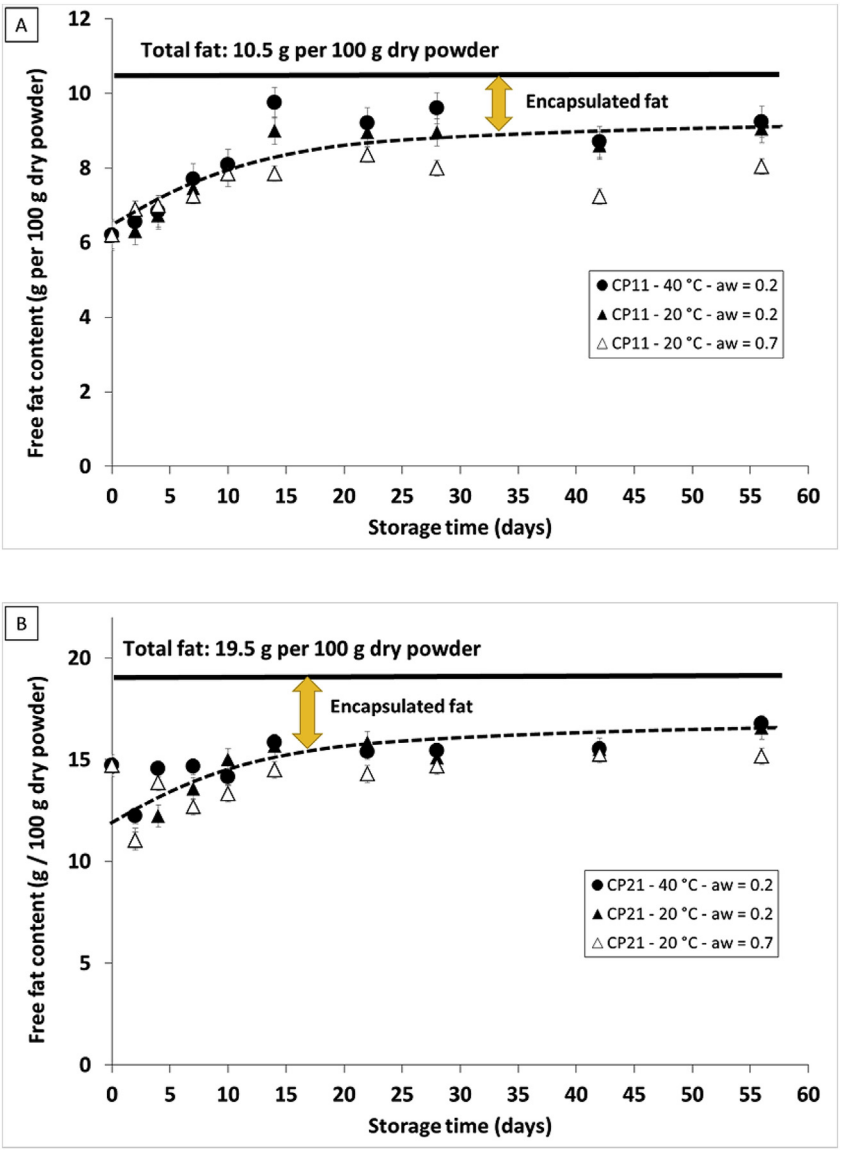

Fig. 5. Evolution of free, encapsulated, and total fat contents of cocoa powders with storage time at 20 (triangles) or 40 °C (circles), and $a_w = 0.2$ (full symbols) or 0.7 (empty symbols). **A**: CP11; **B**: CP21. Straight lines stand for total fat contents, whereas dotted lines were drawn to represent the trends followed by free fat evolutions. When not visible, standard errors were inferior to the marker size.

more contact points and thus are able to form more bridges between them. It was indicated in section 3.2 that caking results of CP11 and CP21 were in agreement with the presumed role of particle shape, but in contradiction with the one of particle size, indicating that the influence of particle shape on caking ability may have surpassed the one of particle size for studied cocoa powders in investigated conditions.

Table 2
XPS surface atomic composition of fresh cocoa powders.

Atoms	Binding Energy (eV)	Surface atomic percentage (%)		
		CP1	CP11	CP21
O_{1s}	532.43 ± 0.03	22.31 ± 0.25	18.20 ± 0.12	16.25 ± 0.13
N_{1s}	399.70 ± 0.05	3.62 ± 0.04	2.61 ± 0.00	1.79 ± 0.05
C_{1s}	284.57 ± 0.03	72.28 ± 0.22	77.65 ± 0.12	80.40 ± 0.05
K_{2p}	292.63 ± 0.08	1.36 ± 0.00	1.21 ± 0.01	1.29 ± 0.04
P_{2p}	133.10 ± 0.09	0.43 ± 0.01	0.33 ± 0.01	0.27 ± 0.00

3.3.2. XPS analysis: focus on particle surface at atomic scale

First, XPS analysis of fresh cocoa powders permitted to relate the atomic and bond composition of powder surface to the presence of proteins, sugars, and fat (Tables 2 and 3). Some CP11 results (N_{1s} and C/O) have ever been presented in a previous work dealing with cocoa powders (Jacquot et al., 2016), but in this study XPS characterisation went one step further by comparing fresh cocoa powders on the basis of surface atomic and bond compositions (Table 2). As XPS analyses on aged powders were performed only once, differences between XPS results were considered statistically significant only if these differences exceeded the highest relative standard error recorded when analysing fresh powders twice, i.e. 3% (value found for CP21 surface nitrogen, cf. Table 2).

From surface atomic composition results, it can be seen that the higher the total fat content, the higher the carbon content and the lower the oxygen and nitrogen contents at the powder surface. Nitrogen content can be related to proteins and minor components such as caffeine and theobromine, because carbohydrates, lipids, and minerals contain negligible amounts of nitrogen. Thus, fewer

Table 3
XPS surface bond composition of fresh cocoa powders.

Bonds	CP1	CP11	CP21
	Surface bond percentage (%)		
C–C(–H)	58.71 ± 0.03	66.56 ± 0.40	68.39 ± 0.27
C–O(–N)	29.77 ± 0.14	23.23 ± 0.73	23.18 ± 0.43
C=O	8.19 ± 0.04	6.74 ± 0.38	4.82 ± 0.00
O–C=O	3.33 ± 0.21	3.47 ± 0.06	3.61 ± 0.16
Ratios			
C/O	3.24 ± 0.04	4.27 ± 0.12	4.95 ± 0.01
$\frac{C-C}{(C-O)+(C=O)+(O-C=O)}$	1.42 ± 0.00	1.99 ± 0.04	2.16 ± 0.03

proteins were located at the surface of fattier powders. As carbohydrates are associated to elevated levels of carbon and oxygen, the combination of carbon content increase and oxygen content decrease when increasing the total fat content of cocoa powders was a sign of increased presence of surface fat and decreased presence of carbohydrates. Mineral content at powder surface seemed not to be greatly affected by total fat content. These results are consistent with the expected greater surface fat coverage of powders richer in fat. Table 2.

Table 3 confirms these observations: from CP1 to CP21, the proportions of C–O(-N), C=O, and O–C=O within C bonds decreased, consistently with the lower contents in surface proteins and carbohydrates. On the contrary, C–C(–H) bonds, which are characteristic for fatty components, significantly increased. Besides, high values of C/O and $\frac{C-C}{(C-O)+(C=O)+(O-C=O)}$ ratios have often been related to high levels of surface fat in food powders (Gaiani et al., 2006, 2007b, 2009). It can be seen in Table 3 that these ratios increased with total fat content, in accordance with the hypothesized increase in surface fat coverage with total fat content.

Now that relevant XPS parameters have been highlighted for the monitoring of surface fat of cacao powders, XPS results during powder storage can be interpreted from the perspective of the role of fat in storage-induced caking of cocoa powder. Fig. 5 displays the evolution of nitrogen content, C–C(H) bond proportion, and C/O ratio for the three investigated cocoa powders during the 56-day ageing study at 40 °C and $a_w = 0.2$. XPS results obtained for storage temperatures of 20 and 30 °C will not be discussed, as no significant caking was observed in these conditions and thus XPS parameters remained mostly stable all along the storage (data not shown). Also, similar evolutions were recorded at $a_w = 0.2$ and 0.7, so it was decided to draw in Fig. 5 the XPS results corresponding to 40 °C storage temperature and 0.2 water activity only.

As for CP1 and CP21, no significant variation (i.e. not exceeding 3%) in XPS results was observed during storage. In particular, nitrogen contents and C/O ratios (Fig. 6A and C) remained constant during 56 days storage at 40 °C. For these powders, the protein content at powder surface was unaffected by storage, which may be an indication that the fat-covered surface area was not significantly modified during storage. Also, the constancy of C/O ratio, which is linked to the relative proportion of fat and carbohydrates at powder surface, confirmed the fact that fat coverage of powder surface remained the same all along the storage for CP1 and CP21. For CP1, this is in accordance with the fact that total, encapsulated, and free fat proportions did not evolve during storage, meaning that CP1 fat coverage and surface stickiness remained weak during storage. For CP21, a conversion of some encapsulated fat into free fat was observed (Fig. 5B), but without significantly changing surface composition of CP21 (Fig. 6B). In fact, powder surface was assumed to be mainly covered by fat from the beginning of powder storage (cf. the very high C/O ratio of fresh CP21 powder in Table 3), thus hindering fat migration to particle surface. It can be deduced that CP21 caking was caused by surface fat already present on powder surface at the beginning of storage. In other words, the free fat released during storage by the opening of closed pores did not significantly change fat coverage of CP21 particle surface, thus the contribution of storage-induced free fat to powder caking remained limited in CP21.

Fig. 6B shows that C–C(–H) bonds slightly increased for CP1 and CP21 after 56 days storage, but this evolution was inferior to XPS accuracy. This was probably due to organic contamination of samples, caused by the exposition of sample surface to air during XPS analysis and leading to a small increase in surface carbon content (Faldt and Bergenstahl, 1994; Kim et al., 2002; Nikolova et al., 2015). In our study, it was logical that the longer the storage time, the more interactions between powder and surrounding air, and the more organic contamination of cocoa particles surface.

For CP11, XPS parameters differently evolved during storage at 40 °C: nitrogen content markedly decreased, whereas C–C(–H) bond proportion and C/O ratio significantly increased. The variations of these parameters were significant from the first ten storage days, consistently with the marked evolution of caking index (Fig. 1B) and free fat content (Fig. 5A) occurring at the same time. This confirms the caking mechanism already evidenced for CP11: some free fat is released during storage by structural reorganisations (due to fat melting and fibre swelling/shrinkage) and migrates toward powder surface if temperature is sufficient (cocoa fat melting occurs between 25 and 35 °C; Jacquot et al., 2016), leading to increased powder surface stickiness and significant caking.

In brief, solvent extraction and XPS results permitted to conclude that CP21 was less sensitive to storage-induced caking than CP11, owing to less free fat released during storage (Fig. 5) and less change in surface fat coverage (Tables 2 and 3, Fig. 6C).

The predominance of the fat melting mechanism in cocoa powder caking was confirmed by TEM observations of powder surface during storage.

3.4. Observation of fat bridging in caked powders by TEM analyses

TEM pictures showed a strong decrease in surface roughness with fat content, a higher surface roughness of CP1 whatever the storage conditions, almost no modifications of surface appearance of CP21 surface during storage, and well-different surface appearances of aged CP11 at 40 °C and at lower temperatures (images not shown for concision purposes). These observations confirmed the previously discussed results, in particular regarding particle size and shape. But it also permitted to give a better insight into the different steps of the caking mechanism occurring during storage of fatty cocoa particles at 40 °C (cf. Fig. 7 and (Jacquot et al., 2016)). Before discussing the implications of TEM observations, it should be highlighted that the double staining of samples performed with uranyl acetate and lead citrate (the latter being often called Reynolds coloration) leads to the formation of a deposit at the surface

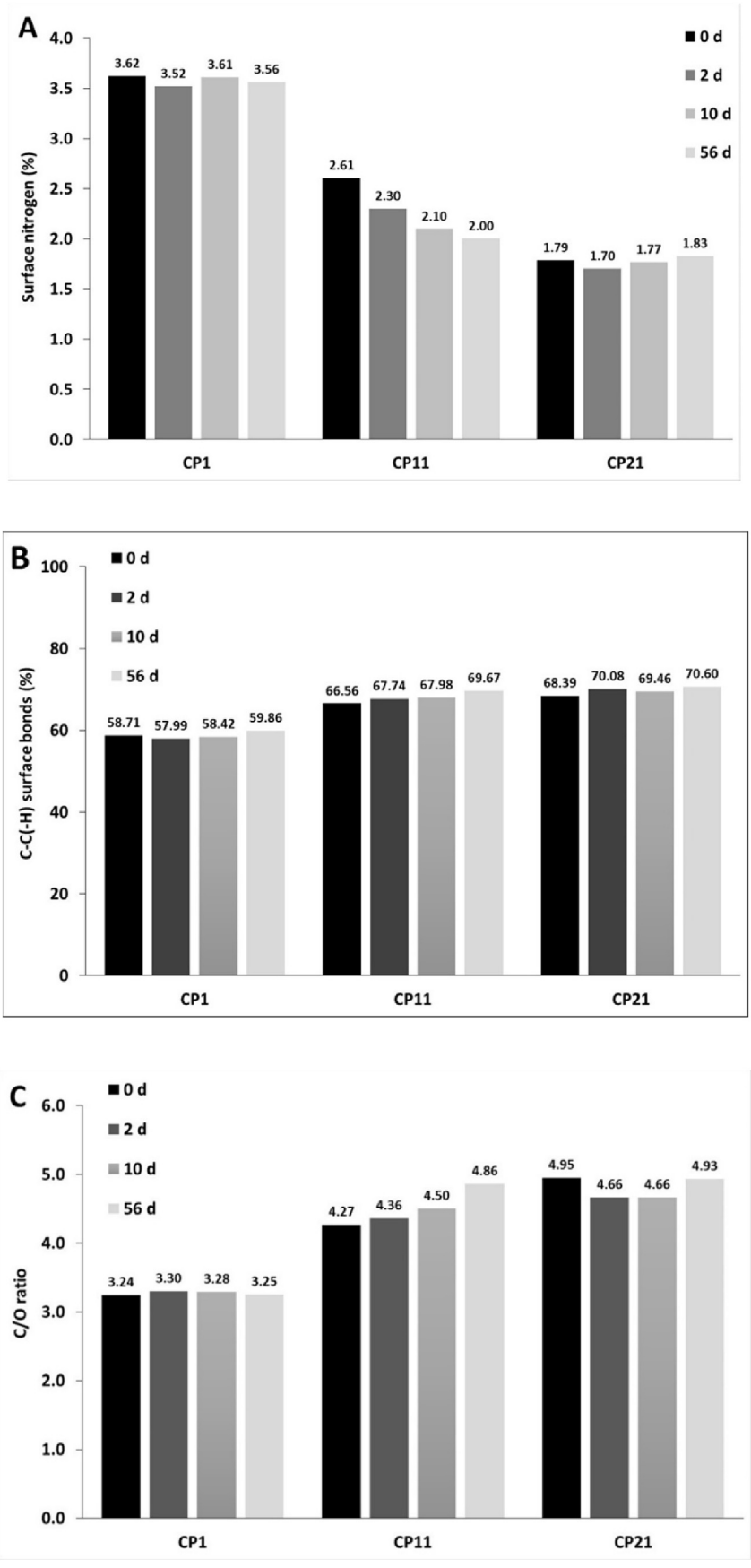

Fig. 6. Evolution of nitrogen content (**A**), C–C(–H) bond proportions (**B**), and C/O ratios (**C**) of CP1, CP11, and CP21 during storage at 40 °C and $a_w = 0.2$.

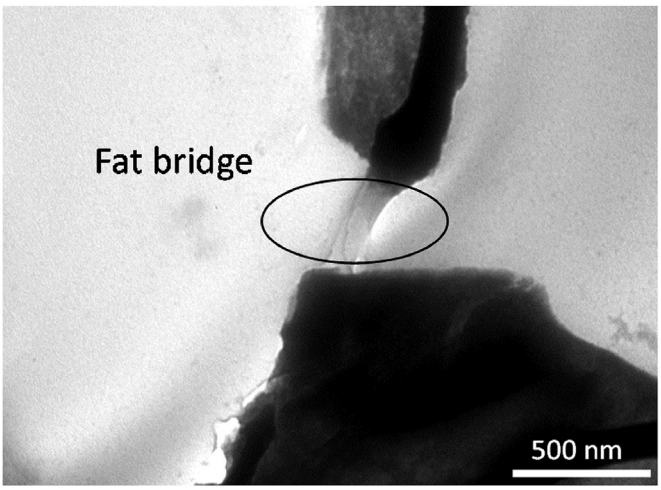

Fig. 7. TEM picture (x 40 000 magnification) of CP11 surface after 56 days storage at 40 °C and $a_w = 0.2$.

of cocoa particles, as uranyl ions mostly interact with proteins and lipids, and lead ions have a higher affinity for proteins and carbohydrates (Reynolds, 1963; Zingsheim and Plattner, 1976). As this double staining absorbs incident beam, dark areas were mostly associated with sample proteins, whereas light areas were generally associated with embedding resin.

Fig. 7 displays a representative example of fat bridge between two adjacent particles: two cocoa particles, appearing in dark on TEM pictures, seemed connected by a thin channel of about 100 nm thickness and 350 nm length that appears in moderate grey on TEM pictures. Caked particles exhibited between their contact points several fat bridges having similar size and shape as in Fig. 7. As the employed double staining particularly highlights proteins but is also sensitive to lipids in a smaller extent (Reynolds, 1963; Zingsheim and Plattner, 1976), this thin channel, appearing in moderate grey, may have a low proteic fraction, and could be mainly constituted of fat. Fat bridging is a necessary step for fat-induced caking, confirming the stated hypothesis of cocoa powder caking driven by the presence of molten fat at cocoa particle surface.

Moreover, this thin fat bridge between contact points of cocoa particles has a typical shape of pendular bridges, i.e. formed by a pendular agglomeration mechanism (Iveson et al., 2001), in which the amount of liquid binder is small. In the current study, the liquid binder is molten fat, which represents a small proportion of cocoa particle matter as showed by solvent extraction analyses (cf. section 3.3.1 and Fig. 5); hence, cocoa particles bound by pendular bridges could be expected as a result of powder caking. The appearance of obtained agglomerates (previously observed by SEM and shown in Jacquot et al., 2016), exhibiting irregular shape and porous structure, is indeed quite similar to the appearance of milk powder agglomerates observed by optical microscopy in Barkouti et al. (2013), confirming the occurrence of pendular agglomeration. The higher apparent compactness of caked cocoa particles shown in Jacquot et al. (2016) in comparison with milk powder agglomerates obtained in an agitated process (Barkouti et al., 2013) is also consistent with the higher proximity of particles during storage.

The mechanism proposed in this study - release of free fat by opening of closed pores (subsequently to fat melting and fibre swelling/shrinkage), fat migration toward particle surface occurring if the temperature is high enough to liquefy lipids, increase in powder surface stickiness, and finally agglomeration of sticking particles leading to powder caking - is consistent with a previous work (Jacquot et al., 2016), in which fat migration in aged fatty cocoa powders was evidenced at 40 °C storage by TEM analysis. In this previous study, the presence of channels from inner pores (presumably enclosed fat globules) to particle surface was evidenced after 2 months storage of CP11 at 40 °C. These channels may allow fat migrating from inner pores to particle surface during storage above the melting points of fatty components, increasing surface stickiness, and inducing the agglomeration of cocoa particles through fat bridges (Fig. 7).

4. Conclusions

Storage-induced caking of cocoa powders has been studied during 56 days by varying powder fat content, temperature, and surrounding air humidity (see Fig. S2 in Supplementary material). Obtained results allowed concluding on the main caking mechanism occurring during cocoa powder ageing. On one hand, experiments performed at different air humidities (20% and 70%) led to similar results, showing no influence of powder water activity. The humidity caking mechanism has then been excluded for cocoa powders. On the other hand, the presence of fat at particle surface and the storage temperature appeared to be the main parameters influencing caking. Indeed, the highest caking indices have been obtained for fatty powders stored at 40 °C. Lower storage temperatures did not induce significant caking. The presence of surface fat is then insufficient to induce caking: surface lipids have to be molten to trigger particle agglomeration, which requires about 25 °C (lower melting point of cocoa lipids). Also, it was evidenced that substantial caking occurs only once all cocoa lipids are molten, i.e. above 36 °C (higher melting point of cocoa lipids). This caking mechanism implies that two particles covered by fat in solid state (for instance fatty cocoa particles at 20 °C) do not significantly stick together. The formation of a liquid fat bridge between particles, followed by solidification of this fat bridge induced by powder cooling, is thus responsible for the caking of cocoa powders. The obtained results are consistent with the fat melting caking mechanism.

Moreover, powder caking increased upon time due to modification of particle structure. The particle size and free fat content increased upon storage, which was related to fat migration toward particle surface, allowed by the formation of channels between enclosed fat globules and particle surface. The opening of enclosed pores may be attributed to structural modifications caused by equilibration with surrounding air humidity of hydrophilic components such as fibres, a major constituent of cocoa powders, or changes in the field of mechanical constrains within cocoa particles owing to thermal expansion of pore-enclosed fat when melting.

Acknowledgements

Nestlé Product Technology Center in Orbe (Switzerland) is thanked for project funding and for the stimulating scientific discussions. The authors present recognition to the LCPME (University of Lorraine, Nancy, France) for XPS measurements. The authors also want to thank Jérôme Chevrier and Justine Paoli (Service Commun de Microscopie, Faculté de Médecine, University of Lorraine, Vandœuvre-lès-Nancy, France) for TEM analyses. Lastly, Carole Perroud (LIBio, University of Lorraine, Vandœuvre-lès-Nancy, France) should also be thanked for her help in developing the sieve analysis protocol.

Appendix A. Supplementary data

Supplementary data related to this article can be found at http://dx.doi.org/10.1016/j.jfoodeng.2016.12.005.

References

Abdi, F., Lakhdar, D., Ibri, K., 2013. Cocoa and health: a study of the cardioprotective effect of cocoa powder on women with hypertension and menaupose. Fundam. Clin. Pharmacol. 27, 28–28.

Afoakwa, E.O., Paterson, A., Fowler, M., 2007. Factors influencing rheological and textural qualities in chocolate: a review. Trends Food Sci. Technol. 18 (6), 290–298.

Aguilera, J.M., del Valle, J.M., Karel, M., 1995. Caking phenomena in amorphous food powders. Trends Food Sci. Technol. 6 (5), 149–155.

Altimiras, P., Pyle, L., Bouchon, P., 2007. Structure–fat migration relationships during storage of cocoa butter model bars: bloom development and possible mechanisms. J. Food Eng. 80 (2), 600–610.

Barkouti, A., Turchiuli, C., Carcel, J.A., Dumoulin, E., 2013. Milk powder agglomerate growth and properties in fluidized bed agglomeration. Dairy Sci. Technol. 93, 523–535.

Bricknell, J., Hartel, R.W., 1998. Relation of fat bloom in chocolate to polymorphic transition of cocoa butter. J. Am. Oil Chemists' Soc. 75 (11), 1609–1615.

Briones, V., Aguilera, J.M., 2005. Image analysis of changes in surface color of chocolate. Food Res. Int. 38 (1), 87–94.

Burgain, J., El Zein, R., Scher, J., Petit, J., Norwood, E.-A., Francius, G., Gaiani, C., 2016. Local modifications of whey proteins isolate powder surface during high temperature storage. J. Food Eng. 178, 39–46.

Calatayud, M., Lopez-de-Dicastillo, C., Lopez-Carballo, G., Velez, D., Munoz, P.H., Gavara, R., 2013. Active films based on cocoa extract with antioxidant, antimicrobial and biological applications. Food Chem. 139 (1–4), 51–58.

Célino, A., Fréour, S., Jacquemin, F., Casari, P., 2014. The hygroscopic behavior of plant fibers: a review. Front. Chem. 1, 43.

Chávez Montes, E., Santamaria, N.A., Gumy, J.-C., Marchal, P., 2011. Moisture induced caking of beverage powders. J. Sci. Food Agric. 91, 2582–2586.

Cimini, A., Gentile, R., Dangelo, B., Benedetti, E., Cristiano, L., Avantaggiati, M.L., Giordano, A., Ferri, C., Desideri, G., 2013. Cocoa powder triggers neuroprotective and preventive effects in a human Alzheimer's disease model by modulating BDNF signaling pathway. J. Cell. Biochem. 114 (10), 2209–2220.

Faldt, P., Bergenstahl, B., 1994. The surface composition of spray-dried protein-lactose powders. Colloids Surfaces A Physicochem. Eng. Aspects 90, 183–190.

Folch, J., Lees, M., Sloane Stanley, G.H., 1957. A simple method for the isolation and purification of total lipids from animal tissues. J. Biol. Chem. 226, 497–509.

Foster, K.D., 2002. The Prediction of Sticking in Dairy Powders. Massey University.

Gaiani, C., Ehrhardt, J.J., Scher, J., Hardy, J., Desobry, S., Banon, S., 2006. Surface composition of dairy powders observed by X-ray photoelectron spectroscopy and effects on their rehydration properties. Colloids Surfaces B-Biointerfaces 49 (1), 71–78.

Gaiani, C., Scher, J., Ehrhardt, J.J., Linder, M., Schuck, P., Desobry, S., Banon, S., 2007a. Relationships between dairy powder surface composition and wetting properties during storage: importance of residual lipids. J. Agric. Food Chem. 55 (16), 6561–6567.

Gaiani, C., Schuck, P., Scher, J., Desobry, S., Banon, S., 2007b. Dairy powder rehydration: influence of protein state, incorporation mode, and agglomeration. J. Dairy Sci. 90 (2), 570–581.

Gaiani, C., Schuck, P., Scher, J., Ehrhardt, J.J., Arab-Tehrany, E., Jacquot, M., Banon, S., 2009. Native phosphocaseinate powder during storage: lipids released onto the surface. J. Food Eng. 94 (2), 130–134.

GEA Niro Research Laboratory, 2003. Analytical Methods Dry Milk Products (Niro Analytical Methods, No. 15 a). Soeborg.

Hartel, R.W., 1999. Chocolate: fat bloom during storage. Manuf. Confect. 79, 89–99.

Hartmann, M., Palzer, S., 2011. Caking of amorphous powders - material aspects, modelling and applications. Powder Technol. 206, 112–121.

Iveson, S.M., Litster, J.D., Hapgood, K., Ennis, B.J., 2001. Nucleation, growth and breakage phenomena in agitated wet granulation processes : a review. Powder Technol. 117, 3–39.

Jacquot, C., Petit, J., Michaux, F., Chavez, E., Dupas, J., Girard, V., Gianfrancesco, A., Scher, J., Gaiani, C., 2016. Cocoa powder surface composition during aging: a focus on fat. Powder Technol. 292, 195–202.

James, B.J., Smith, B.G., 2009. Surface structure and composition of fresh and bloomed chocolate analysed using X-ray photoelectron spectroscopy, cryo-scanning electron microscopy and environmental scanning electron microscopy. Lwt-Food Sci. Technol. 42 (5), 929–937.

Kim, E.H.-J., Chen, X.D., Pearce, D., 2002. Surface characterization of four industrial spray-dried dairy powders in relation to chemical composition, structure and wetting property. Colloids Surfaces B Biointerfaces 26, 197–212.

Le Brun, O., Scher, J., Fasquel, J.-P., Hardy, J., 2006. Quantification du mottage de poudres alimentaires: comparaison de méthodes (food powder caking: methods of comparison). Sci. des Aliments 26, 271–287.

Lonchampt, P., Hartel, R.W., 2006. Surface bloom on improperly tempered chocolate. Eur. J. Lipid Sci. Technol. 108 (2), 159–168.

Murrieta-Pazos, I., Gaiani, C., Galet, L., Calvet, R., Cuq, B., Scher, J., 2012a. Food powders: surface and form characterization revisited. J. Food Eng. 112 (1–2), 1–21.

Murrieta-Pazos, I., Gaiani, C., Galet, L., Scher, J., 2012b. Composition gradient from surface to core in dairy powders: agglomeration effect. Food Hydrocoll. 26 (1), 149–158.

Nikolova, Y., Petit, J., Sanders, C., Gianfrancesco, A., Desbenoit, N., Frache, G., Francius, G., Scher, J., Gaiani, C., 2014. Is it possible to modulate the structure of skim milk particle through drying process and parameters? J. Food Eng. 142, 179–189.

Nikolova, Y., Petit, J., Sanders, C., Gianfrancesco, A., Scher, J., Gaiani, C., 2015. Toward a better determination of dairy powders surface composition through XPS matrices development. Colloids Surfaces B Biointerfaces 125, 12–20.

Omobuwajo, T.O., Busari, O.T., Osemwegie, A.A., 2000. Thermal agglomeration of chocolate drink powder. J. Food Eng. 46, 73–81.

Peschar, R., Pop, M.M., De Ridder, D.J., van Mechelen, J.B., Driessen, R.A., Schenk, H., 2004. Crystal structures of 1, 3-distearoyl-2-oleoylglycerol and cocoa butter in the β (V) phase reveal the driving force behind the occurrence of fat bloom on chocolate. J. Phys. Chem. B 108 (40), 15450–15453.

Reynolds, E.S., 1963. The use of lead citrate at high pH as an electron opaque stain in electron microscopy. J. Cell Biol. 17, 208.

Svanberg, L.N., Lorén, N., et al., 2012. Chocolate swelling during storage caused by fat or moisture migration. J. Food Sci. 77 (11), 328–334.

Talbot, G., 1999. Industrial Chocolate Manufacture and Use. Beckett, Oxford.

Tietz, R.A., Hartel, R.W., 2000. Effects of minor lipids on crystallization of milk fat-cocoa butter blends and bloom formation in chocolate. J. Am. Oil Chemists' Soc. 77 (7), 763–771.

Vignolles, M.L., Jeantet, R., Lopez, C., Schuck, P., 2007. Free fat, surface fat and dairy powders: interactions between process and product. A review. Lait 87 (3), 187–236.

Wille, R., Lutton, E., 1966. Polymorphism of cocoa butter. J. Am. Oil Chem. Soc. 43 (8), 491–496.

Zingsheim, H.P., Plattner, H., 1976. Electron microscopic methods in membrane biology. In: Korn, E.D. (Ed.), Methods in Membrane Biology. Plenum Press, New York, pp. 47–48.